Industrial-era lead and mercury contamination in southern Greenland implicates North American sources

Marta Pérez-Rodríguez [1,2 *], Noemí Silva-Sánchez [1], Malin E. Kylander [3,4], Richard Bindler [5], Tim M. Mighall [6], J. Edward Schofield [6], Kevin J. Edwards [6,7,8], Antonio Martínez Cortizas [1]

[1] Departamento de Edafoloxía e Química Agrícola, Facultade de Bioloxía, Universidade de Santiago de Compostela, Campus Sur, Santiago de Compostela 15782, Spain

[2]Institut für Geoökologie, AG Umweltgeochemie, Technische Universität Braunschweig, 38106 Braunschweig Germany

[3] Department of Geological Sciences, Stockholm University, SE-10691 Stockholm, Sweden

[4] The Bolin Centre for Climate Research, Stockholm University, SE-10691 Stockholm, Sweden

[5] Department of Ecology and Environmental Sciences, Umeå University, SE-901 87 Umeå, Sweden

[6] Department of Geography and Environment, School of Geosciences, University of Aberdeen, Elphinstone Road, Aberdeen AB24 3UF, UK

[7] Department of Archaeology, School of Geosciences, University of Aberdeen, Elphinstone Road, Aberdeen AB24 3UF, UK

[8] Clare Hall, University of Cambridge, Herschel Road, Cambridge CB3 9AL, UK

* Corresponding Author:

E-mail: m.perez-rodriguez@tu-bs.de

Current address: Institute of Geoecology - Division of Environmental Geochemistry, Langer Kamp 19c R303B, 38106 Braunschweig Phone: (+) 49-(0)531-391-7242

Abstract

To study the long-range transport of atmospheric pollutants from lower latitude industrial areas to the Arctic, we analysed a peat core spanning the last ~700 cal. yr (~AD 1300-2000) from southern Greenland, an area sensitive to atmospheric pollution from North American and Eurasian sources. A previous investigation conducted in the same location recorded atmospheric lead (Pb) pollution after ~1845, with peak values recorded in the 1970s, and concluded that a North American source was most likely. To confirm the origin of the lead, we present new Pb isotope data from Sandhavn, together with a high-resolution record for mercury (Hg) deposition. Results demonstrate that the mercury accumulation rate has steadily increased since the beginning of the 19th century, with maximum values of 9.3 μg m^{-2} yr^{-1} recorded ~1940. Lead isotopic ratios show two mixing lines: one which represents inputs from local and regional geogenic sources, and another that comprises regional geogenic and pollution sources. Detrending the Pb isotopic ratio record (thereby extracting the effect of the geogenic mixing) has enabled us to reconstruct a detailed chronology of metal pollution. The first sustained decrease in Pb isotope signals is recorded as beginning ~1740-1780 with the lowest values (indicating the highest pollution signature) dated to ~1960-1970. The ^{206}Pb/^{207}Pb ratio of excess Pb (measuring 1.222, and reflecting pollution-generated Pb), when compared with the Pb isotopic composition of the Sandhavn peat record since the 19th century and the timing of Pb enrichments, clearly points to the dominance of pollution sources from North America, although it did not prove possible to further differentiate the emissions sources geographically.

Key words: Hg; Pb isotopes; peat, metal pollution; isotopic residuals; atmospheric deposition

1. INTRODUCTION

The Arctic, including Greenland (Figure 1), has experienced significant human impacts through the effects of long-range atmospheric transport of pollutants since ancient times. The oldest evidence of atmospheric metal pollution in Greenland dates back to the Carthaginian and Roman periods, and is attested to by an increase in lead (Pb) concentrations between 680 BC and AD 193 measured in the Summit ice core (Hong et

al., 1994). This was accompanied by a change in the Pb isotopic composition that suggested the source of pollution was from Spanish ores (Rosman et al., 1997). Evidence of medieval lead pollution in Greenland, dating to the 15th century AD, has been proposed using inverse modelling on data obtained from Lake Igaliku in southern Greenland (Massa et al., 2015). Before that study was conducted, no significant changes in the modern levels of atmospheric metal deposition had been identified prior to the 18th century AD in Greenland (Bindler et al., 2001b; Candelone et al., 1995; Michelutti et al., 2009; Murozumi et al., 1969; Rosman et al., 1994; Silva-Sánchez et al., 2015).

Most investigations into long-range atmospheric pollution in Greenland consider the Pb content and isotopic ratios in ice cores and lake sediments. By contrast, there are fewer records available for the accumulation of other heavy metals such as mercury (Hg). An increase in Hg content since the Industrial Revolution has been demonstrated in Greenlandic marine and lake sediments, as well as ice cores (Asmund and Nielsen, 2000; Bindler et al., 2001a; Dommergue et al., 2016; Faïn et al., 2009; Lindeberg et al., 2006), and the associated risks for Arctic wildlife and human populations have been highlighted (AMAP, 2011). Very few of these investigations have produced Hg records that extend into the pre-industrial era. Consequently our understanding of the long-term accumulation of Hg in the Greenlandic environment remains relatively poor.

In addition to some contribution from local sources, a long-distance origin is accepted for atmospheric pollutants recorded in Greenland (Skov et al., 2016). Whilst the existence of a wide range of pollution origins existing simultaneously is likely (such as North America, Europe and Asia), strong control on atmospheric pollutant transport is exerted by seasonal Arctic and Subarctic air masses (Sturges and Barrie, 1989a). The polar front is not zonally symmetrical and can extend as far south as ~40º N over Eurasia in January, thus making northern Eurasia the major source region for air pollution transport into the Arctic (Law and Stohl, 2007). As such, results from recent snow and atmospheric aerosols collected from the Canadian High Arctic (Shotyk et al., 2005a; Sturges and Barrie, 1989b) pointing to a Eurasian source of Pb are noteworthy. It seems unusual, therefore, that the Pb pollution signal recorded at CF8 (Easter Baffin Island) has a US origin (Michelutti et al., 2009).

The high elevation of the Greenland Ice Sheet and its location in the high Arctic leave it more greatly exposed to atmospheric pollution from distant sources than the rest of the Arctic (Stohl, 2006). Thus, in snow samples collected from the Summit Station in central Greenland, the analysis of the Pb isotopic composition of layers dating to ~AD 1967-1989 indicated that the USA was a prevalent source of Pb aerosols during the 1970s, decreasing in relative importance into the late 1980s (Rosman et al., 1994, 1993). In the same study (Rosman et al., 1993), and in a subsequent investigation in south Greenland (Rosman et al., 1998), seasonal changes in pollution sources were identified: North American sources were predominant during winter and autumn, while during spring and summer the sources were mainly located in the North Atlantic region, northern and western Europe, and in the Arctic Basin.

In contrast to the ice cores, which come from high elevation locations and receive pollutants transported in the high troposphere, geochemical studies of peat cores and lake sediments have been undertaken at lower altitudes in near-coastal areas in southwestern and southern Greenland (Bindler et al., 2001a, 2001b; Shotyk et al., 2003). These depositional contexts do not show consistent enrichment through metal pollution prior to the 18th century, and the identification of emissions sources for these locations has also proved to be problematic. In lake sediments from Kangerlussuaq (southwestern Greenland), the application of a simple isotopic mixing model suggested that the Pb record had a mainly Western European origin (Bindler et al., 2001b), whereas lake sediments from Pearyland (northern Greenland) demonstrate a Eurasian source (Michelutti et al., 2009). A peat record from Tasiusaq (southern Greenland) indicates a 20th century North American pollution source (Shotyk et al., 2003), although the complex isotopic composition of the signal warranted a cautious interpretation.

More recently, a multiproxy study conducted at an ombrotrophic mire at Sandhavn, southern Greenland, has provided firm evidence for Pb enrichment beginning ~AD 1845 (Silva-Sánchez et al., 2015). This record is important because the location of the site – near the southern tip of Greenland – places it at the edge of the Arctic front. The region also experiences a bimodal wind direction with a strong probability of observing both westerly and easterly high speed aeolian events (Moore et al., 2008; Renfrew et al., 2008). The chronology of Pb pollution, which was closer in timing to the events of the North American Industrial Revolution (Kylander et al., 2004; Norton et al., 1997) than

to that within Europe, together with the presence of long-distance transported pollen (Rousseau et al., 2003) and cryptotephras (Blockley et al., 2015), supports a hypothesis that northeastern North America was the probable source of the Pb (Silva-Sánchez et al., 2015). In this paper we extend the geochemical investigations of this site through the measurement of stable Pb isotopes along with total Hg. Our aims are (i) to compare the Pb record with that of another likely long-range atmospheric metal pollutant, *viz.* Hg, and (ii) to use Pb isotope analysis to provide a more precise identification of the source area(s) for atmospheric pollutants arriving in south Greenland.

2. MATERIAL AND METHODS

2.1 Location and sampling

Sandhavn (59°59.9'N, 44°46.6'W) is located on the coast of Greenland approximately 50 km northwest of Cape Farewell, the most southerly point on the island (Figure 1). The climate is subarctic, with cold winters and cool summers (JJA mean ~6 ºC), moderate annual precipitation (~900 mm per annum), and frequent strong winds. During the late medieval period (~AD 1000-1400) the site was inhabited by the Norse and the Thule Inuit. Today it lies abandoned, 35 km to the northwest of the nearest major settlement (the small town of Nanortalik; ~1,400 inhabitants). Open oceanic heath overlying podzolic soils is characteristic of the local area. The regional geology comprises gneisses and granites of the Ketilidian mobile belt with basic and intermediate intrusions (Allaart, 1976), with granites and gabbros forming the local lithologies (Figure 1). The site is described in further detail elsewhere (Golding et al., 2014, 2011; Raahauge et al., 2002; Silva-Sánchez et al., 2015).

In August 2008, a peat monolith (40 cm) was recovered from a small (~30 m diameter) basin (59° 59.875'N, 44 °46.637'W) adjacent to the former homefields and Norse ruins at Sandhavn (Figure 1). The sediment column was collected in a monolith tin from the open face of a pit dug into the mire. The field stratigraphy comprised a base of saturated coarse grey-brown sands (40-36 cm) overlain by an orange-brown *turfa* (rootlet) peat containing abundant bryophytes (36-5 cm). The top of the profile (5-0 cm) contained the (living) root mat, which was not analyzed for geochemistry. The monolith was wrapped in polythene and returned to the University of Aberdeen, where it was kept refrigerated (4°C) prior to sub-sampling in the laboratory. In preparation for

geochemical analysis, the core was cut into 1 cm thick slices and samples were dried and milled to a fine powder with an agate mill. Only the basal sands and the peat unit (40-5 cm) were analyzed.

2.2 Chronology

An age-depth model for the peat monolith was developed by Silva-Sanchez *et al.* (2015) (reproduced here as Figure 2) and we adopt the same chronology. What follows is a brief summary. For detailed discussion of the development of the model, the reader is referred to the earlier paper.

The model uses *Clam* software to fit a smoothed-spline through a series of calibrated AMS ^{14}C and ^{210}Pb dates. The model applies to only the organic section of the profile (0–36 cm), including the living root mat, with errors varying between ±2 cal. yr (smallest towards the surface) and ±50 cal. yr (greatest towards the base). It indicates that peat formation began ~AD 1270 and was continuous thereafter, with notably slow accumulation rates (0.020-0.025 cm yr^{-1}) occurring during ~AD 1400-1800 – a period encapsulating much of the Little Ice Age (LIA) – followed by accelerated peat growth during warmer conditions in the 19th and particularly the 20th centuries. The calendar dates cited in this paper for events at Sandhavn are 'best' estimates drawn from the model, and all dates referred to in years AD.

2.3 Sample preparation and analysis

Samples were dried at room temperature (25 ºC) until they reached a constant weight and were then analysed for stable Pb isotopes and total Hg. The analyses were done on the same samples as those measured during the previous work at the same site (Silva-Sánchez et al., 2015).

2.3.1 Lead isotope analyses

Peat samples were ashed at 450°C overnight to remove any organic matter. The remaining residues were digested using an acid mixture of HNO_3 and HF contained within closed digestion vessels in a MARS-Xpress microwave system (CEM, Mattheus, USA). A ratio of 0.16 ml HF to 50 mg ash was determined to be the correct mixture required to digest the samples (Kylander et al., 2004). After digestion, samples were dried and Pb was isolated by ion exchange chromatography (Weiss et al., 2004).

Isotopic measurements were determined using an *IsoProbe* Multi Collector-Inductively Coupled Plasma-Mass Spectrometer (MC-ICP-MS) (Micromass, Manchester, UK) at the Naturhistorika Riksmuseet, Sweden. The instrument was equipped with a CETAC desolvator and a T1H concentric nebuliser for introducing the sample. Seven independently adjustable Faraday cups in static mode were used for isotope ratio measurements. Averaged acid blank intensities were subtracted from raw intensities to correct for Faraday cup offset and instrumental and solvent blanks. Corrections for Hg interference on ^{204}Pb were typically ≤0.1%. Instrumental mass bias was corrected by spiking samples with NIST-SRM 977 Tl to Pb/Tl ratio of 2:1 and using optimised Tl ratios and the exponential law (see Weiss et al. [2004] for details).

Procedural blanks were <1% of the total Pb in the samples. The repeatability and accuracy of Pb isotope measurements are based on multiple measurements (n=23) of NIST-SRM 981 Pb acquired during the week long measurement session. Precision (2σ) on individual Pb isotope ratios expressed relative to the mean (in ppm) is: 299 for ^{206}Pb/^{204}Pb, 388 for ^{207}Pb/^{204}Pb, 543 for ^{208}Pb/^{204}Pb and 230 for ^{206}Pb/^{207}Pb. The accuracy as evaluated against values published by Galer and Abouchami (1998) also expressed relative to the mean are (in ppm): 50 for ^{206}Pb/^{204}Pb, 462 for ^{207}Pb/^{204}Pb, 210 for ^{208}Pb/^{204}Pb and 509 for ^{206}Pb/^{207}Pb.

2.3.2 Isotopic mixing model

For distinguishing between separate Pb sources, we use three isotopes plots (e.g. ^{206}Pb/^{208}Pb vs. ^{206}Pb/^{207}Pb or ^{207}Pb/^{204}Pb vs. ^{208}Pb/^{204}Pb). The basic equation of a binary mixing model could be re-expressed to calculate the excess Pb isotope ratio with the objective of inferring extra information of mixing. This value for a given sample is the isotope ratio required for an additional source of Pb to cause an observed change in the isotope signature of the sample relative to a background value or to some reference value prior to a major shift in the isotope signature. We estimated the mean isotopic composition of the excess ^{206}Pb/^{207}Pb contribution for the Sandhavn samples (i.e. pollution Pb) after Farmer et al. (1996):

$$^{206}Pb/^{207}Pb_{excess} = \frac{(Pb_{sample} \times {}^{206}Pb/^{207}Pb_{sample}) - (Pb_{ref} \times {}^{206}Pb/^{207}Pb_{ref})}{Pb_{sample} - Pb_{ref}}$$

where $^{206}Pb/^{207}Pb_{sample}$ refers to the isotope ratio and Pb_{sample} refers to the total Pb concentration of a given sample, and $^{206}Pb/^{207}Pb_{ref}$ and Pb_{ref} refer to the mean isotope ratio and concentration, respectively, of peat background values.

2.3.2 Mercury analysis

The analyses for total Hg were done using a Milestone DMA-80 analyser. As a control, measurements were replicated for one in every five samples, and a standard reference material of the moss *Pleurozium schreberi* (Steinnes et al., 1997), M3, was run with each set of samples. The quantification limit was 1.7 ng g^{-1} and mean recovery was 97 ± 1.2%. The mean difference between sample replicates was 3.4% (range 0.4-16.1%).

3. RESULTS AND DISCUSSION

3.1 Lead and lead isotopes

Lead concentrations remain below 2.5 μg g^{-1} throughout most of the peat record (from 35 cm to the top) and progressively increase above 22 cm (Figure 3). Maximum Pb concentrations (16.4–19.6 μg g^{-1}) were reached between 10 -14 cm, with the overlying sediments characterized by a progressive decrease in values. As Silva-Sánchez et al., (2015) noted, lead does not share any significant covariation with the lithogenic elements (e.g. Ti, Zr) in the Sandhavn core. To remove contributions of geogenic Pb from local dust (i.e. generated from erosion of local soils) from the peat record and isolate the atmospheric Pb pollution signal, values were normalized against titanium (Ti, as indicator of erosion), and Pb/Ti ratios were used as a proxy for atmospheric Pb pollution. Although the patterns of Pb concentrations and Pb/Ti ratios are similar, some minor differences were detected, mainly between ~1900 and 1940, when some of the Pb seems to be linked with increased soil erosion caused by the return of sheep farming to the region in the early 20th century (Silva-Sánchez et al., 2015).

The depth profile of $^{206}Pb/^{207}Pb$ (Figure 3) may be divided into three sections separated by abrupt transitions. In the basal sand (40-36 cm) values are low (1.167 ± 0.074), with a peak (1.298) at 37.5 cm. Above the sand-peat contact (36 cm) the ratio increases with high values (1.307 ± 0.029) recorded between 33.5-21.5 cm. The ratio then decreases, becoming near-constant (1.187± 0.009) in the upper 21 cm.

Three isotope plots were produced to examine changes in Pb sources and to assign possible mixing end members (Figure 4). There are three end members that correspond to the main sections identified in the isotopic record (as described above), and the data suggest two mixing lines. The first of these – labeled as the geological mixing line, M-I on Figure 4 – includes the basal sand (low radiogenic signature) and the peat samples overlying this up to a depth of 22 cm (the most radiogenic values). The second (pollution mixing) line – M-II on Figure 4 – involves the peat samples measured above 22 cm (also see section 3.4 for further details).

Because the basal samples have lower radiogenic signatures (bottom – left section of three isotopes plot, Figure 4), –they overlap some of the samples considered to be contaminated by pollutants, making it difficult to establish the departure from the geological mixing to the pollution mixing line and thus fix accurately the start of significant atmospheric Pb pollution in the Sandhavn peat record. To address the problem we applied a mathematical approach based on the calculation of the Pb isotope residuals between the trajectory of the unpolluted trend (geological mixing line, M-I) and the observed values over the past two centuries (pollution mixing line, M-II). Thus, we calculated the regression function of each of the two mixing lines (M-I and M-II) thus estimating the statistical relationship among variables (i.e. isotopic ratios) for each mixing line. The equation of M-I is expressed for $^{206}Pb/^{207}Pb$ and $^{206}Pb/^{208}Pb$ as:

(1)

$$Expected_{\frac{206}{208}sample} = m \times Observed^{206}Pb/^{207}Pb_{sample} + n$$

where *m* and *n* are the slope and the y-intercept (respectively) of the linear regression of $^{206}Pb/^{208}Pb$ to $^{206}Pb/^{207}Pb$ of unpolluted samples. Then, we determined the difference between the observed isotopic values and the expected ones according to the geological mixing line (M-I), i.e. the residuals.

(2)

$$Residual_{\frac{206}{207}vs\frac{206}{208}} = Obseved^{206}Pb/^{208}Pb_{sample} - Expected_{\frac{206}{208}sample}$$

The residuals close to zero (from basal sand samples pre-dating ~1740, Figure 5C) confirm that the observed values are best placed on the geogenic mixing line.When residuals increasingly depart from zero and move away from this mixing line they indicate a greater influence from pollution sources (thereby reflecting samples post-dating ~1740-1780). The beginning of atmospheric Pb pollution in Sandhavn varies slightly according to which residuals are used. It is considered to be between 1740 and 1780 according to the residuals of Pb^{206}/Pb^{207} *vs.* Pb^{208}/Pb^{204} and Pb^{206}/Pb^{208} *vs.* Pb^{206}/Pb^{207}, but later (~1800) according to the residuals of Pb^{207}/Pb^{204} *vs.* Pb^{208}/Pb^{204}. These dates are more than 100 years apart when comparing the $^{206}Pb/^{204}Pb$ and $^{206}Pb/^{207}Pb$ ratios (see decreases in isotope trend Figure 5B) although both are before the rise of Pb/Ti (~1845). However, the main decrease in isotopic values, associated with the increased in pollution signature is fixed – based on residuals and isotopic ratios (Figure 5 B and C, respectively) – to just before 1900, and is also similar to the increases in Pb/Ti ratios (Figure 5A).

3.2 Mercury

Mercury concentrations varied from 9 to 28 ng g^{-1} in the basal sandy sediment (40–36 cm) and from 47 to 297 ng g^{-1} in the peat (<36 cm). From 36 cm (the base of the peat) to 14.5 cm, concentrations rise (from 60 to 297 ng g^{-1}) with an abrupt increase from 20.5 cm, peaking at 14.5 cm (Figure 3); from 14.5 to 5.5 cm, values decrease with a slight upturn at 7.5 cm (140 ng g^{-1}). Organically bound elements such as Hg can be enriched by the effect of peat mineralization (Biester et al., 2003; Martínez Cortizas et al., 2007); however, no significant correlation with peat decomposition proxies based on FTIR data (Silva-Sánchez et al., 2015) have been found (Figure S1). Additionally, although peat growth and carbon (C) accumulation rates appear to have been lower during the inferred Spörer and Maunder solar minima (Silva-Sánchez et al., 2015), Hg concentrations were not affected.

To account for the effects of changes in peat density and accumulation rate on geochemical concentrations, and to enable direct comparison of figures with previous studies, Hg accumulation rates are reported. Background accumulation rates for Hg recorded in the Sandhavn core (Figure 5) occur from the start of peat accumulation (~AD 1270, 35.5 cm) until ~1800 (23.5 cm), with values through this period lower than 1.0 μg m^{-2} yr^{-1} (depth values referred to Figure 3). These low values are similar to those (< 3.0 μg m^{-2} yr^{-1}) reported for other pre-industrial peat and lake sediments records (Bindler et al., 2001a, 2001b; Shotyk et al., 2003) from south and southwestern Greenland. A gradual increase during the industrial period occurs from ~1800 to 1880 (23.5–20.5 cm) when Hg accumulation rates change significantly, reaching a maximum (9.3 μg m^{-2} yr^{-1}) by ~1940 (16.5 cm) (Figure 5). Thereafter Hg accumulation rates decline, corresponding to the general pattern for this element observed elsewhere in the Northern Hemisphere (Bindler et al., 2001a; Martínez Cortizas et al., 2012; Norton et al., 1997; Shotyk et al., 2003). The continuous decrease up until 1980 is a bit slower at ~1960 (14.5 cm), with an accumulation rate of 6.7 μg m^{-2} yr^{-1}. A secondary peak (3.8 μg m^{-2} yr^{-1}) is evident around 1987 (7.5 cm) and appears to coincide with the enrichment in Hg measured in ice and snow samples from the high Arctic during the late 1980s and 1990s (Zheng, 2015).

The maximum Hg accumulation rate in the Sandhavn core (6-10 μg m^{-2} yr^{-1}) is similar to that recorded at Lakes 53 and 70 (Bindler et al., 2001a) located ~850 km north of Kangerlussuaq Fjord. In contrast, the maximum Hg accumulation rate reported from the only other Greenland peatland core study published to date (Shotyk et al., 2003) is 16–17 times higher (164 μg m^{-2} yr^{-1}) than that at Sandhavn or the aforementioned lakes, although these values have been considered unrealistic (Bindler, 2006). Similarly, maxima from European and North American records that lie in closer proximity to major emission sources are all higher, for example: Dumme Mosse mire in Sweden (~25 μg m^{-2} yr^{-1}) (Bindler, 2003); four ombrotrophic bogs from Scotland (51–85 μg m^{-2} yr^{-1}) (Farmer et al., 2009); Chao de Lamoso bog in NW Spain (27–60 μg m^{-2} yr^{-1}) (Martínez Cortizas et al., 2012); Arlberg bog (Minnesota, US; 38 ± 11 μg m^{-2} yr^{-1}) (Benoit et al., 1994); and Caribou Bog (Maine, US; 32 μg m^{-2} yr^{-1}) (Roos-Barraclough et al., 2006).

The low Hg accumulation rates observed at Sandhavn may be explained in two ways. Firstly, Sandhavn is located at great distance from any major sources of Hg pollution emanating from North America and Europe. Secondly, rates of peat accumulation, and the decomposition of organic matter at Sandhavn, were limited in the period ~AD 1400-1800 (Silva-Sánchez et al., 2015) – encompassing much of the LIA – at least when compared with peatlands from mid-latitudes. Consequently, the latter may have been more affected by enrichment in Hg, most likely driven by intense peat mineralisation (Martínez Cortizas et al., 2007). Both reasons point towards the suitability of Sandhavn, and probably other similarly remote cold high latitude environments, as sensitive archives for long-distance transported pollution given that the effect of peat post-depositional processes (i.e. organic matter decomposition) is reduced in these locations.

3.3 Chronology of Hg and Pb pollution in southernmost Greenland

3.3.1. Pre-pollution period to 1900

Both the metals studied at Sandhavn show different patterns of change over time. Figure 5 shows the chronology for the Pb isotope ratio and residuals, Pb/Ti ratios (as determined by Silva-Sánchez et al., 2015), and Hg accumulation rates. While Pb/Ti ratios (Figure 5) were low and constant until ~1845, the start of Hg pollution in the Sandhavn record began earlier (from ~1780) and precedes the former by ~65 years. However, when the information provided by the lead isotopic residuals is considered (section 3.1), the beginning of lead pollution may be fixed between 1740 and 1800. The first major decrease in the isotope residuals occurs ~1740–1780 and continues until ~1885; this is partly in accord with the main change in Pb isotope ratios recorded in the Nunatak lake sediment record, southwestern Greenland (Bindler et al., 2001b), even though the changes in the latter began earlier (~1700). The date for the onset of lead pollution at Sandhavn according to the residuals is slightly earlier than that shown by the increase in Hg and Pb/Ti but is consistent with other studies that suggest modern metal pollution in Greenland had begun prior to the 19th century (Bindler et al., 2001a; Massa et al., 2015). Although the decline in Pb isotope residuals seems to start at ~1700 (26.5 cm), the values are not systematically lower than the previous period until 1740-1780.

Mercury and lead pollution records in Sandhavn during this period may be connected to patterns in the burning of wood and coal in North America (Figure 6). The increase in Hg accumulation rates at Sandhavn match estimates of the use of wood as an energy source in USA (Figure 6), which show a progressive and continuous increase from the end of the 18th. Similarly, it seems that the beginning of the use of coal in North America, between 1850 and 1900, had a strong impact of Hg and Pb pollution records in south Greenland. The first major rise in coal consumption in the USA (~1860) coincides with a slight increase in Hg accumulation and with the first signs of Pb atmospheric pollution as indicated by the rise in Pb/Ti ratios and the decline in the Pb residual values (Figure 6). Thus, the progressive intensification in coal consumption in the USA and Canada (the first estimations in Canada date back to 1880, Figure 6) runs in parallel with the increase in metal accumulation in Sandhavn. However, due to the long lifetime of gaseous elemental Hg in the atmosphere and its transport and deposition on a global scale (Slemr et al., 1985), it is necessary to consider that other sources may also contribute to the increase in Hg accumulation in southern Greenland. The comparison of our Hg record with an atmospheric Hg global simulation (Figure 6) shows a similar rise until 1900 which, accordingly to the models, was mainly caused by gold mining (Horowitz et al., 2014; Streets et al., 2011).

3.3.1. From 1900 to 1990

Mercury and Pb increase significantly during the 19th century but reach their peak values at different times (~1940–1950 and ~1980, respectively). In the case of Hg, this is in agreement with other pollution records from Greenland (Boutron et al., 1998) and North America (Beal et al., 2015; Roos-Barraclough et al., 2006). Even allowing for differences in the type, location and resolution of the records, the peak in Hg pollution at Sandhavn compares favorably with values measured in snow (Boutron et al., 1998) and a recent model based on firn air data (Faïn et al., 2009) from Summit Station. However, these maxima are slightly earlier than the peak in the worldwide and US production of Hg (U.S Geological Survey, 2014), an indirect indicator of anthropogenic Hg emissions to the atmosphere (Figure 6).

The slow reduction in Hg pollution during 1962–1968 at Sandhavn despite the temporal decrease in coal burning in North America could be due to an increase in global Hg consumption in commercial products like paint, batteries and in chlor-alkali plants (Horowitz et al., 2014) (Figure 6). However, this does not rule out the Hg contribution

433 from coal burning after 1950 (Streets et al., 2011). Considering these, it is especially
434 noteworthy that the maximum Hg accumulation in Sandhavn corresponds to a rebound
435 in coal consumption in North America (both in the USA and in Canada). The
436 subsequent decline (after 1970) and peak around 1990 has been related to Hg
437 consumption by chlor-alkali plants (Horowitz et al., 2014).
438
439 A recent reconstruction (modelled) of atmospheric gaseous elemental mercury in the
440 Arctic shows a slightly different scenario; an increase since the 1950s peaking in the
441 late 1960s and early 1970s, and a return to low concentrations around 1995-2000
442 (Dommergue et al., 2016). The difference in our results compared to those generated by
443 Dommergue et al. (2016) (Figure 6) may be due to the core location for the latter being
444 ~2000 km further north than Sandhavn, and elevated (77°N and 2452 m asl), which
445 might result in different source areas for Hg.
446
447 The record of Pb pollution at Sandhavn, as shown by the Pb/Ti ratio and Pb isotopic
448 residuals, seem to be related with energy production in North America. A decrease in
449 the residuals starts ~1908, and this is simultaneous with the sharp increase in metal
450 pollution shown in the Sandhavn core and in other Greenland records (Bindler et al.,
451 2001a, 2001b). The increase in Pb from atmospheric deposition in Sandhavn seems to
452 reflect the increase of coal consumption as well as the beginning and progressive
453 increase in petroleum consumption, especially after 1940 following the introduction of
454 leaded gasoline. The lowest residual values (i.e. the highest Pb pollution signal
455 indicated by the isotopes) are dated to the 1940s and 1970s, and agree with data
456 obtained from analysis of the Summit ice cores (Faïn et al., 2009; Rosman et al., 1994).
457 The fall in gasoline Pb consumption in the USA since 1970, declining ~80% by the
458 early 1980s (Nichols, 1997), probably contributed to the pronounced increase in
459 isotopic residual values from ~1979 (Figure 6). A slight drop in Sandhavn isotopic
460 residuals in ~1988 indicates an increase in the pollution signal. Similar patterns are also
461 reported by the Pb isotopic composition in ice and snow samples from the high Arctic
462 (Shotyk et al., 2005b), where authors attribute the modern inputs of anthropogenic Pb to
463 other industrial sources. The absence of samples more modern than 1990 (the last
464 sample) in the Sandhavn core, prevents an examination of the most recent trends. The
465 close agreement between the isotopic residuals chronology and data from other archives

indicates that it is an appropriate and precise method to determine changes in the chronology of the Pb isotopic signature.

3.4 Sourcing

Although the ratios involving the four stable Pb isotopes (^{204}Pb, ^{206}Pb, ^{207}Pb and ^{208}Pb) were determined (Figure 3) and used to construct three-isotope plots (Figure 4), the identification of potential sources is based on the ^{206}Pb/^{207}Pb and ^{206}Pb/^{208}Pb ratios, because these are the most commonly reported in Pb pollution studies. As such there are more end members defined for comparison.

In Figure 7, the isotopic composition of the Sandhavn samples is compared with other published isotopic data from Greenland (Andersen, 1997; Colville et al., 2011; Kalsbeek and Taylor, 1985; Rosman et al., 1997; Shotyk et al., 2003; Taylor et al., 1992; Whitehouse et al., 2005), North America (Bollhöfer and Rosman, 2001; Graney et al., 1995) and Europe (Dunlap et al., 1999; Farmer et al., 2002; Shotyk et al., 2005; Weiss et al., 1999). Samples from the sandy basal sediments of the Sandhavn core have a fairly uniform isotopic composition (^{206}Pb/^{207}Pb 1.118-1.143 and ^{206}Pb/^{208}Pb 0.479-0.488; Figures 7 and 4) that is similar to that found in rocks from the Archaean craton in southwest and southeast Greenland (Taylor et al., 1992; Whitehouse et al., 2005) (Figure 7). There is one sample (37.5 cm, Figure 3) with an isotopic signature closer to a second (potential) source (1.298 and 0.53, ^{206}Pb/^{207}Pb and ^{206}Pb/^{208} ratios respectively). Pre-industrial peat samples (~AD 1300 to the late ~1800s; upper right in Figure 7) have a more radiogenic composition (^{206}Pb/^{207}Pb 1.312 ± 0.028, ^{206}Pb/^{208}Pb 0.536 ± 0.009) than most of the samples from the base of the core. They fall close to the geogenic mixing line, between the Sandhavn basal sands (derived from the local geological material) and rocks of the Ketilidian Mobile Belt of southern Greenland (Andersen, 1997; Colville et al., 2011; Kalsbeek and Taylor, 1985) that could generate a regional geological dust signal. Values assigned to geogenic Pb (peat residue – geogenic lead; Figure 7) in a minerogenic peat record from Tasiusaq (southern Greenland) (Shotyk et al., 2003), located 150 km northwest of Sandhavn, are also on the same geogenic mixing line and support the interpretation of a regional southern Greenland Pb source.

Peat samples dating to the Industrial period (from the end of the 1800s forwards) define a second (pollution) mixing line that ranges from the regional geological signal to

values typical of pollution sources ($^{206}Pb/^{207}Pb$ 1.178 and $^{206}Pb/^{208}Pb$ 0.483, lower radiogenic values). Data from the peat core from Tasiusaq (southern Greenland) (Shotyk et al., 2003) show a similar transition between regional pre-industrial values and the pollution signal (leachate – atmospheric Pb; Figure 7). At Sandhavn, the low isotopic ratios are similar to the anthropogenic signal found in lake records from the USA for the period 1972-1978 (Graney et al., 1995) (e.g. Lake Erie sediment – anthropogenic signal; Figure 7) and show the same trend as that seen in Pb in atmospheric data collected in Canada during the mid- to late 1990s from eastern Canada, namely, Newfoundland, Labrador, and Chicoutimi, Quebec, respectively (Bollhöfer and Rosman, 2001) (Air – Newfoundland and Chicoutimi, 1994-1999; Figure 7).

There is a large difference in the isotopic signature between Pb ores used in the USA and Canada. Coal in the USA used for industrial purposes from 1900 to 1920 was extracted from deposits in West Virginia and Pennsylvania and displays $^{206}Pb/^{207}Pb$ values in the range 1.18-1.21(Graney et al., 1995). In the 1960s, the highly radiogenic Missouri ores with a $^{206}Pb/^{207}Pb$ ratio of ~1.28-1.32 dominated industrial use (Shirahata et al., 1980) and the Pb used in gasoline in the USA was taken from the similarly radiogenic Mississippi Valley type ores ($^{206}Pb/^{207}Pb$, >1.22) (Wu and Boyle, 1997). In contrast, the most important Pb ores used by industry in eastern Canada (Quebec, Ontario and New Brunswick) are less radiogenic, with $^{206}Pb/^{207}Pb$ ratios of 1.15-1.16 (Blais, 1996). The $^{206}Pb/^{207}Pb$ signature of gasoline in eastern Canada was 1.16 during the 1980s. Less radiogenic Pb has been found in British Columbia ores in western Canada ($^{206}Pb/^{207}Pb$ 1.05) (Sturges and Barrie, 1987). Nonetheless, lake sediments from northeastern Canada showed that US contributions to the total Pb burden in surficial lake sediments are often in excess of 50%, with an increasingly Canadian Pb industrial isotopic signal further north (Blais, 1996). At Sandhavn, the Industrial era peat samples (Figure 7) are similar to the anthropogenic signal extracted from Lake Erie in sediments dating from 1940 to 1989 and the pollution mixing trend shown by air samples collected in eastern Canada (Lake Erie sediment and Newfoundland & Chicoutimi, respectively, inset Figure 4).

Based upon the results obtained from previous research that suggested Europe to be the main emissions source for atmospheric lead transported to western Greenland (Bindler

et al., 2001b), we have collated lead isotopic data from European records (peat and moss samples) covering the last 300 years as well as modern air data (Figure 7) in order to compare this with our own results. The resulting mixing line shows a different trajectory to those previously discussed for Sandhavn (Figure 4) due to the different lead sources. The isotopic composition of Pb mined and used in western Europe from ancient times 1.16 – 1.21 Pb^{206}/Pb^{207} (see Rosman et al., [1997]) and references therein) – with similar values for coal – dominate the mixing until the early 20^{th} century. Thereafter the more radiogenic signature (1.04 Pb^{206}/Pb^{207}) of British Columbia-type ores enters into the European pollution mixing as the alkyls-Pb additive for gasoline, leading to the lowering of the Pb isotope pollution signature in contrast to ratios for the USA (Figure 7)

Taken together, these data indicate that metal pollution at Sandhavn was mainly influenced by sources from the North America, given that the Pb isotopic signatures also differ from those of Europe (see European mixing line, Figure 7). However separating between emissions sources in the USA and Canada is not possible, mainly due to the complexity of regional and local mixing along with the variability of sources to be considered and their relative change over time (i.e. coal and petroleum from different ores).

As mentioned, we estimated the mean isotopic composition of the excess $^{206}Pb/^{207}Pb$ contribution for the Sandhavn samples (Farmer et al., 1996). As background values (1.321 $^{206}Pb/^{207}Pb$ ratio, 0.96 μg g^{-1} Pb concentration) we used those in Pre-industrial peat samples (~1500 to 1650), and calculated excess Pb values for samples dating to the period after ~1800 (Industrial era). The average isotopic value of the excess Pb was 1.193 (±0.074) that is well above the numerical levels determined for lakes in southwestern Greenland (1.145) (Bindler et al., 2001b) and aerosols from the high Canadian Arctic (~1.160) (France and Blais, 1998), but closer to the upper limit of European signals (~1.14 – 1.20, reported in [Bindler et al., 2001b]) and the lower limit of the isotope field for pollution sourced in the US (1.19 – 1.25) (Rosman et al., 1994; Shirahata et al., 1980; Sturges et al., 1993). Taking into account that the isotopes residuals' chronology suggests that Pb pollution started ~1740–1780, the recalculated excess $^{206}Pb/^{207}Pb$ contribution including these samples (1.222 ± 0.114) may point to a

567 significant influence of Pb pollution from the USA in southernmost Greenland,
568 although the results are not conclusive.
569
570 We do not have direct evidence for the origin of Hg, but according to the Pb isotope
571 results we would expect the main source for Hg contamination to be also from the USA.
572 However, Hg has a complex behaviour in the environment. Its relatively long residence
573 time in the atmosphere (1 year) favours long-range transport and homogenization at a
574 hemispheric scale, making it more difficult to determine its precise origin. More than a
575 decade of research demonstrates that Hg isotopes could be used to trace sources, as well
576 as biogeochemical cycling and reactions involving Hg (Blum et al., 2014). The
577 combined analyses of Pb and Hg (both concentration and isotopic composition) may
578 provide the means to assist further in the identification of such pollution sources in
579 northern latitudes.
580
581
582 **Acknowledgments**
583 We would like to thank Jesús R. Aboal (Universidade de Santiago de Compostela) and
584 Kjell Billström (Naturhistoriska Riksmuseet) for access to the laboratory facilities;
585 Antonio Rodríguez López helped with laboratory work. This research was done under
586 the framework of the projects CGL2010-20672 (Plan Nacional I+D+i, Spanish
587 Ministerio de Economía y Competitividad), R2014/001 and GPC2014-009 (Dirección
588 Xeral I+D, Xunta de Galicia). The authors gratefully acknowledge the financial support
589 of the UK Leverhulme Trust *Footprints on the Edge of Thule* programme award for
590 core collection and associated environmental research.
591
592 **Figure captions**
593
594 **Figure 1.** (A) The location of Sandhavn (black star) and other places mentioned in the
595 text. Key to labels: A Summit ice cores (Rosman et al., 1997, 1994, 1993); B rock
596 samples from Kangerdlugssuaq (Taylor et al., 1992); C peat record in Tasiusaq,
597 Greenland (Massa et al., 2015; Shotyk et al., 2003); D Akilia rocks, Greenland
598 (Whitehouse et al., 2005); E lake sediments, Lake 53 and Lake 16, SW Greenland
599 (Bindler et al., 2001a, 2001b); F peat record from the Faroe Islands (Shotyk et al.,
600 2005); G *Sphagnum* moss samples from Scotland (Farmer et al., 2002); H peat record

from Denmark (Shotyk et al., 2003); I peat core from Schöpfenwaldmoor, Switzerland (Weiss et al., 1999); J & K lake sediments from Lake Ontario and Lake Erie (Graney et al., 1995); L & N aerosols samples from Chicoutimi and Newfoundland, Canada (Bollhöfer and Rosman, 2001); M peat record from Caribou bog, US (Roos-Barraclough et al., 2006); O peat records, Norway (Dunlap et al., 1999); P lake sediments, Lake CF8 Baffin Island (Michelutti et al., 2009); Q snow samples from Devon Island (Shotyk et al., 2005b); R peat records from NW Spain (Martínez Cortizas et al., 2012); S rock samples from south Greenland (Andersen, 1997; Colville et al., 2011; Kalsbeek and Taylor, 1985); T peat record from southern Sweden (Bindler, 2003). (B) Location of the study area (boxed) within Greenland. (C) Simplified geological map of the area around Sandhavn (data from GEUS, 2017).

Figure 2. Age-depth model for the monolith, taken from(Silva-Sánchez et al., 2015).

Figure 3. Hg and Pb concentrations and accumulation rates through the Sandhavn monolith and lead isotopic ratio Pb^{206}/Pb^{207}.

Figure 4. Lead (Pb) isotope scatterplots of the Sandhavn samples.

Figure 5. Main variables used in this study through the peat at Sandhavn (~AD 1300-2000). (A) Hg accumulation rates (green line), Pb/Ti (blue line) (Silva-Sánchez et al., 2015); (B) Pb isotopes ratios and, (C) an Pb isotope residuals Pb^{206}/Pb^{208} *vs.* Pb^{206}/Pb^{207} (continuous line); Pb^{206}/Pb^{204} *vs*. Pb^{208}/Pb^{204} (dotted line) and Pb^{207}/Pb^{204} *vs.* Pb^{208}/Pb^{204} (dashed line). Grey line indicates zero Pb isotopic residuals (i.e. the values are the expected for the geogenic mixing line, see the text).

Figure 6. Detailed record showing the period after ~1790 for the Sandhavn variables discussed in the text. Data of US. energy consumption attributed to sources in the USA (in Quadrillion Btu) (US Energy Information Administration, 2012) is indicated using different scales for wood, coal and petroleum respectively. Canadian energy consumption (Quirin, 2014) is expressed in thousands of barrels (petroleum) and in thousands of tons (coal). Pb isotope residuals correspond to Pb^{206}/Pb^{208} *vs* Pb^{206}/Pb^{207} values and the red line indicates residuals equal to zero. Mercury world production and Hg apparent consumption (data from the U.S. Geological Survey, 2014) are expressed

in tons (t) with different scales. Data for global simulated atmospheric Hg was extracted from Horowitz et al., (2014) and Arctic simulated GEM (gaseous elemental Hg) from Dommergue et al., (2016).

Figure 7. Scatterplots comparing the lead isotopic composition of the samples from Sandhavn against data from Greenland, North America and West Europe. The type of sample and the sampling location is indicated in the legend. (CN: Canada; DE: Denmark; FA: Faroe Island; GL: Greenland; NO: Norway; SW: Sweden; SW: Switzerland; UK: United Kingdom; US: United States). Lettering (A-S) corresponds with the locations marked on Figure 1. References: A (Rosman et al., 1997); B (Taylor et al., 1992); C (Shotyk et al., 2003); D (Whitehouse et al., 2005); G (Farmer et al., 2002); I (Weiss et al., 1999); J & K (Graney et al., 1995); L & N (Bollhöfer and Rosman, 2001); M (Shotyk et al., 2005); O (Dunlap et al., 1999); S (Andersen, 1997; Colville et al., 2011; Kalsbeek and Taylor, 1985)).

Supporting Information

Figure S1. Scatterplot of Hg concentrations against proxies of peat decomposition measured by Silva-Sánchez et al., (2015) (PC1o, left panel; PC3o, right panel) in the Sandhavn record. The p-values of Pearson's test are 0.09 and 0.88 respectively.

Table S1. Mean (Avg), standard deviation (Sd), maximum (Max) and minimum (Min) values for mercury, lead and lead isotope ratios through the Sandhavn monolith.

References

Allaart, J.H., 1976. Ketilidian mobile belt in South Greenland, in: Escher, A., Stuart-Watt, W. (Eds.), Geology of Greenland. Geological Survey of Greenland Copenhagen, pp. 120–151.

AMAP, A., 2011. Assessment 2011: mercury in the Arctic, Arctic Monitoring and Assessment Programme (AMAP). Oslao, Norway. doi:10.1017/CBO9781107415324.004

Andersen, T., 1997. Age and petrogenesis of the Qassiarsuk carbonatite-alkaline silicate volcanic complex in the Gardar tift, South Greenland. Mineral. Mag. 61, 499–513. doi:10.1180/minmag.1997.061.407.03

Asmund, G., Nielsen, S., 2000. Mercury in dated Greenland marine sediments. Sci.

669 Total Environ. 245, 61–72. doi:10.1016/S0048-9697(99)00433-7
670 Beal, S., Osterberg, E.C., Zdanowicz, C., Fisher, D., 2015. An ice core perspective on
671 mercury pollution during the past 600 years. Environ. Sci. Technol. 49, 7641–
672 7647. doi:10.1021/acs.est.5b01033
673 Benoit, J.M., Fitzgerald, W.F., Damman, A.W.H., 1994. Historical atmospheric
674 mercury deposition in the mid-continental US as recorded in an ombrotrophic peat
675 bog. Mercur. Pollut. Integr. Synth. 187–202.
676 Biester, H., Martinez-Cortizas, a., Birkenstock, S., Kilian, R., 2003. Effect of Peat
677 Decomposition and Mass Loss on Historic Mercury Records in Peat Bogs from
678 Patagonia. Environ. Sci. Technol. 37, 32–39. doi:10.1021/es025657u
679 Bindler, R., 2006. Mired in the past — looking to the future: Geochemistry of peat and
680 the analysis of past environmental changes. Glob. Planet. Change 53, 209–221.
681 doi:10.1016/j.gloplacha.2006.03.004
682 Bindler, R., 2003. Estimating the natural background atmospheric deposition rate of
683 mercury utilizing ombrotrophic bogs in Southern Sweden. Environ. Sci. Technol.
684 37, 40–46. doi:10.1021/es020065x
685 Bindler, R., Renberg, I., Appleby, P.G., Anderson, N.J., Rose, N.L., 2001a. Mercury
686 Accumulation Rates and Spatial Patterns in Lake Sediments from West Greenland:
687 A Coast to Ice Margin Transect. Environ. Sci. Technol. 35, 1736–1741.
688 doi:10.1021/es0002868
689 Bindler, R., Renberg, I., John Anderson, N., Appleby, P.G., Emteryd, O., Boyle, J.,
690 2001b. Pb isotope ratios of lake sediments in West Greenland: inferences on
691 pollution sources. Atmos. Environ. 35, 4675–4685. doi:10.1016/S1352-
692 2310(01)00115-7
693 Blais, J.M., 1996. Using Isotopic Tracers in Lake Sediments To Assess Atmospheric
694 Transport of Lead in Eastern Canada. Water. Air. Soil Pollut. 92, 329–342.
695 Blockley, S.P.E., Edwards, K.J., Schofield, J.E., Pyne-O'Donnell, S.D.F., Jensen,
696 B.J.L., Matthews, I.P., Cook, G.T., Wallace, K.L., Froese, D., 2015. First evidence
697 of cryptotephra in palaeoenvironmental records associated with Norse occupation
698 sites in Greenland. Quat. Geochronol. 27, 145–157.
699 doi:10.1016/j.quageo.2015.02.023
700 Blum, J.D., Sherman, L.S., Johnson, M.W., 2014. Mercury Isotopes in Earth and
701 Environmental Sciences. Annu. Rev. Earth Planet. Sci. 42, 249–269.
702 doi:10.1146/annurev-earth-050212-124107

703 Bollhöfer, A., Rosman, K.J.R., 2001. Isotopic source signatures for atmospheric lead:
704 The Northern Hemisphere. Geochim. Cosmochim. Acta 65, 1727–1740.
705 doi:10.1016/S0016-7037(00)00630-X
706 Boutron, C.F., Vandal, G.M., Fitzgerald, W.F., Ferrari, P., 1998. A forty year record of
707 mercury in central Greenland snow in snow deposited Greenland reported from
708 previous studies of Greenland snow by major Combined probably plagued by
709 major contamination problems during estimated contributions from natural Hg
710 sources. Goephysical Res. Lett. 25, 3315–3318.
711 Candelone, J.-P., Hong, S., Pellone, C., Boutron, C.F., 1995. Post-Industrial Revolution
712 changes in large-scale atmospheric pollution of the northern hemisphere by heavy
713 metals as documented in central Greenland snow and ice. J. Geophys. Res. 100,
714 16605. doi:10.1029/95JD00989
715 Colville, E.J., Carlson, A.E., Beard, B.L., Hatfield, R.G., Stoner, J.S., Reyes, A. V,
716 Ullman, D.J., 2011. Sr-Nd-Pb isotope evidence for ice-sheet presence on southern
717 Greenland during the Last Interglacial. Science (80-.). 333, 620–623.
718 doi:10.1126/science.1204673
719 Dommergue, A., Martinerie, P., Courteaud, J., Witrant, E., Etheridge, D., 2016. A new
720 reconstruction of atmospheric gaseous elemental mercury trend over the last 60
721 years from Greenland firn records. Atmos. Environ. 136, 156–164.
722 doi:10.1016/j.atmosenv.2016.04.012
723 Dunlap, C.E., Steinnes, E., Flegal, A.R., 1999. A synthesis of lead isotopes in two
724 millennia of European air. Earth Planet. Sci. Lett. 167, 81–88. doi:10.1016/S0012-
725 821X(99)00020-5
726 Faïn, X., Ferrari, C.P., Dommergue, A., Albert, M.R., Battle, M., Severinghaus, J.,
727 Arnaud, L., Barnola, J.-M., Cairns, W., Barbante, C., Boutron, C., 2009. Polar firn
728 air reveals large-scale impact of anthropogenic mercury emissions during the
729 1970s. Proc. Natl. Acad. Sci. U. S. A. 106, 16114–16119.
730 doi:10.1073/pnas.0905117106
731 Farmer, J.G., Anderson, P., Cloy, J.M., Graham, M.C., MacKenzie, A.B., Cook, G.T.,
732 2009. Historical accumulation rates of mercury in four Scottish ombrotrophic peat
733 bogs over the past 2000 years. Sci. Total Environ. 407, 5578–5588.
734 doi:10.1016/j.scitotenv.2009.06.014
735 Farmer, J.G., Eades, L.J., Atkins, H., Chamberlain, D.F., 2002. Historical trends in the
736 lead isotopic composition of archival Sphagnum mosses from Scotland (1838-

737 2000). Environ. Sci. Technol. 36, 152–157. doi:10.1021/es010156e
738 Farmer, J.G., Eades, L.J., Mackenzie, A.B., Kirika, A., Bailey-Watts, T.E., 1996. Stable
739 Lead Isotope Record of Lead Pollution in Loch Lomond Sediments since 1630
740 A.D. Environ. Sci. Technol. 30, 3080–3083. doi:10.1021/es960162o
741 France, R.L., Blais, J.M., 1998. Lead concentrations and stable isotopic evidence for
742 transpolar contamination of plants in the Canadian High Arctic. Ambio 27, 506–
743 508.
744 Galer, S.J.G., Abouchami, W., 1998. Practical application of lead triple spiking for
745 correction of instrumental mass discrimination. Miner. Mag. A 62, 491–492.
746 Golding, K.A., Simpson, I.A., Schofield, J.E., Edwards, K.J., 2011. Norse–Inuit
747 interaction and landscape change in southern Greenland? A geochronological,
748 Pedological, and Palynological investigation. Geoarchaeology 26, 315–345.
749 doi:10.1002/gea.20351
750 Golding, K.A., Simpson, I.A., Wilson, C.A., Lowe, E.C., Schofield, J.E., Edwards, K.J.,
751 2014. Europeanization of Sub-Arctic Environments: Perspectives from Norse
752 Greenland's Outer Fjords. Hum. Ecol. 43, 61–77. doi:10.1007/s10745-014-9708-y
753 Graney, J.R., Halliday, A., N., Keeler, G.J., Nriagu, J.O., Robbins, J.A., Norton, S.A.,
754 1995. Isotopic record of lead pollution in lake sediments from the northeastern
755 United States. Geochim. Cosmochim. Acta 59, 1715–1728. doi:10.1016/0016-
756 7037(95)00077-D
757 Hong, S., Candelone, J.-P., Patterson, C.C., Boutron, C.F., 1994. Greenland ice
758 evidence of hemispheric lead pollution two millennia ago by Greek and Roman
759 civilizations. Science (80-.). 265, 1841–1843.
760 Horowitz, H.M., Jacob, D.J., Amos, H.M., Streets, D.G., Sunderland, E.M., 2014.
761 Historical mercury releases from commercial products: Global environmental
762 implications. Environ. Sci. Technol. 48, 10242–10250. doi:10.1021/es501337j
763 Kalsbeek, F., Taylor, P.N., 1985. Isotopic and chemical variation in granites across a
764 Proterozoic continental margin—the Ketilidian mobile belt of South Greenland.
765 Earth Planet. Sci. Lett. 73, 65–80. doi:10.1016/0012-821X(85)90035-4
766 Kylander, M.E., Weiss, D.J., Jeffries, T., Coles, B.J., 2004. Sample preparation
767 procedures for accurate and precise isotope analysis of Pb in peat by multiple
768 collector (MC)-ICP-MS. J. Anal. At. Spectrom. 19, 1275–1277.
769 Law, K.S., Stohl, A., 2007. Arctic Air Pollution: Origins and Impacts. Science (80-.).
770 315, 1537–1540. doi:10.1126/science.1137695

771 Lindeberg, C., Bindler, R., Renberg, I., Emteryd, O., Karlsson, E., Anderson, N.J.,
772 2006. Natural Fluctuations of Mercury and Lead in Greenland Lake Sediments.
773 Environ. Sci. Technol. 40, 90–95. doi:10.1021/es051223y
774 Martínez Cortizas, A., Biester, H., Mighall, T., Bindler, R., 2007. Climate-driven
775 enrichment of pollutants in peatlands. Biogeosciences 4, 905–911. doi:10.5194/bg-
776 4-905-2007
777 Martínez Cortizas, A., Peiteado Varela, E., Bindler, R., Biester, H., Cheburkin, A.,
778 2012. Reconstructing historical Pb and Hg pollution in NW Spain using multiple
779 cores from the Chao de Lamoso bog (Xistral Mountains). Geochim. Cosmochim.
780 Acta 82, 68–78. doi:10.1016/j.gca.2010.12.025
781 Massa, C., Monna, F., Bichet, V., Gauthier, É., Losno, R., Richard, H., 2015. Inverse
782 modeling of past lead atmospheric deposition in South Greenland. Atmos. Environ.
783 105, 121–129. doi:10.1016/j.atmosenv.2015.01.025
784 Michelutti, N., Simonetti, A., Briner, J.P., Funder, S., Creaser, R.A., Wolfe, A.P., 2009.
785 Temporal trends of pollution Pb and other metals in east-central Baffin Island
786 inferred from lake sediment geochemistry. Sci. Total Environ. 407, 5653–62.
787 doi:10.1016/j.scitotenv.2009.07.004
788 Moore, G.W.K., Pickart, R.S., Renfrew, I.A., 2008. Buoy observations from the
789 windiest location in the world ocean, Cape Farewell, Greenland. Geophys. Res.
790 Lett. 35, 3–7. doi:10.1029/2008GL034845
791 Murozumi, M., Chow, T.J., Patterson, C., 1969. Chemical concentrations of pollutant
792 lead aerosols, terrestrial dusts and sea salts in Greenland and Antarctic snow strata.
793 Geochim. Cosmochim. Acta 33, 1247–1294. doi:10.1016/0016-7037(69)90045-3
794 Nichols, A.L., 1997. Lead in Gasoline, in: Morgenstern, R.D. (Ed.), Economic Analyses
795 at EPA: Assessing Regulatory Impact. Resources for the Future, Washington DC,
796 pp. 49–86.
797 Norton, S.A., Evans, G.C., Kahl, J.S., 1997. Comparison of Hg and Pb fluxes to
798 hummocks and hollows of ombrotrophic Big Heath Bog and to nearby Sargent Mt.
799 Pond, Maine, USA. Water, Air, Soil Pollut. 100, 271–286.
800 doi:10.1023/a:1018380610893
801 Quirin, G.D., 2014. Statistics Canada. Section Q : Energy and Electric Power.
802 Raahauge, K., Appelt, M., Gulløv, H.C., Kapel, H., Krause, C., Møller, N.A., 2002.
803 Tidlig Thulekultur i Stydgrønland (Early Thule culture in South Greenland). Rapp.
804 om undersøgelserne i Nanortalik Kommune, sommeren 2001.

805 Renfrew, I.A., Moore, G.W.K., Kristjánsson, J.E., Ólafsson, H., Gray, S.L., Petersen,
806 G.N., Bovis, K., Brown, P.R.A., Føre, I., Haine, T., Hay, C., Irvine, E.A.,
807 Lawrence, A., Ohigashi, T., Outten, S., Pickart, R.S., Shapiro, M., Sproson, D.,
808 Swinbank, R., Woolley, A., Zhang, S., 2008. The Greenland flow distortion
809 experiment. Bull. Am. Meteorol. Soc. 89, 1307–1324.
810 doi:10.1175/2008BAMS2508.1
811 Roos-Barraclough, F., Givelet, N., Cheburkin, A.K., Shotyk, W., Norton, S.A., 2006.
812 Use of Br and Se in peat to reconstruct the natural and anthropogenic fluxes of
813 atmospheric Hg: A 10000-year record from Caribou Bog, Maine. Environ. Sci.
814 Technol. 40, 3188–3194. doi:10.1021/es051945p
815 Rosman, K.J.R., Chisholm, W., Boutron, C.F., Candelone, J.P., Gorlach, U., 1993.
816 Isotopic evidence for the source of lead in Greenland snows since the late 1960s.
817 Nature 362, 333–335.
818 Rosman, K.J.R., Chisholm, W., Boutron, C.F., Candelone, J.P., Hong, S., 1994. Isotopic
819 evidence to account for changes in the concentration of lead in Greenland snow
820 between 1960 and 1988. Geochim. Cosmochim. Acta 58, 3265–3269.
821 doi:10.1016/0016-7037(94)90054-X
822 Rosman, K.J.R., Chisholm, W., Boutron, C.F., Candelone, J.P., Jaffrezo, J.L.,
823 Davidson, C.I., 1998. Seasonal variations in the origin of lead in snow at Dye 3,
824 Greenland. Earth Planet. Sci. Lett. 160, 383–389. doi:10.1016/S0012-
825 821X(98)00098-3
826 Rosman, K.J.R., Chisholm, W., Hong, S., Candelone, J.P., Boutron, C.F., 1997. Lead
827 from Carthaginian and Roman Spanish mines isotopically identified in Greenland
828 ice dated from 600 B.C. to 300 A.D. Environ. Sci. Technol. 31, 3413–3416.
829 doi:10.1021/es970038k
830 Rousseau, D.-D., Duzer, D., Cambon, G., Jolly, D., Poulsen, U., Ferrier, J., Schevin, P.,
831 Gros, R., 2003. Long distance transport of pollen to Greenland. Geophys. Res.
832 Lett. 30, 10–13. doi:10.1029/2003GL017539
833 Shirahata, H., Elias, R.W., Patterson, C.C., Koide, M., 1980. Chronological variations
834 in concentrations and isotopic compositions of anthropogenic atmospheric lead in
835 sediments of a remote subalpine pond. Geochim. Cosmochim. Acta 44, 149–162.
836 Shotyk, W., Goodsite, M.E., Roos-Barraclough, F., Frei, R., Heinemeier, J., Asmund,
837 G., Lohse, C., Hansen, T.S., 2003. Anthropogenic contributions to atmospheric
838 Hg, Pb and As accumulation recorded by peat cores from southern Greenland and

839 Denmark dated using the 14C “bomb pulse curve.” Geochim. Cosmochim. Acta
840 67, 3991–4011. doi:10.1016/S0016-7037(03)00409-5
841 Shotyk, W., Goodsite, M.E., Roos-Barraclough, F., Givelet, N., Le Roux, G., Weiss, D.,
842 Cheburkin, A.K., Knudsen, K., Heinemeier, J., van Der Knaap, W., Norton, S. a.,
843 Lohse, C., 2005. Accumulation rates and predominant atmospheric sources of
844 natural and anthropogenic Hg and Pb on the Faroe Islands. Geochim. Cosmochim.
845 Acta 69, 1–17. doi:10.1016/j.gca.2004.06.011
846 Shotyk, W., Zheng, J., Krachler, M., Zdanowicz, C., Koerner, R., Fisher, D., 2005a.
847 Predominance of industrial Pb in recent snow (1994-2004) and ice (1842-1996)
848 from Devon Island, Arctic Canada. Geophys. Res. Lett. 32, 1–4.
849 doi:10.1029/2005GL023860
850 Shotyk, W., Zheng, J., Krachler, M., Zdanowicz, C., Koerner, R., Fisher, D., 2005b.
851 Predominance of industrial Pb in recent snow (1994–2004) and ice (1842–1996)
852 from Devon Island, Arctic Canada. Geophys. Res. Lett. 32, 21814.
853 doi:10.1029/2005GL023860
854 Silva-Sánchez, N., Schofield, J.E., Mighall, T.M., Martínez Cortizas, A., Edwards, K.J.,
855 Foster, I., 2015. Climate changes, lead pollution and soil erosion in south
856 Greenland over the past 700 years. Quat. Res. 84, 159–173.
857 doi:10.1016/j.yqres.2015.06.001
858 Skov, H., Bossi, R., Massling, A., Sørensen, L.-L., Nøjgaard, J.K., Christensen, J.,
859 Hansen, K.M., Jensen, B., Glasius, M., 2016. Atmospheric Pollution Research on
860 Greenland, in: Kallenborn, R. (Ed.), Implications and Consequences of
861 Anthropogenic Pollution in Polar Environments. Springer Berlin Heidelberg,
862 Berlin, Heidelberg, pp. 21–39. doi:10.1007/978-3-642-12315-3_3
863 Slemr, F., Schuster, G., Seiler, W., 1985. Distribution, speciation, and budget of
864 atmospheric mercury. J. Atmos. Chem. 3, 407–434. doi:10.1007/BF00053870
865 Steinnes, E., Rühling, Å., Lippo, H., Mäkinen, A., 1997. Reference materials for large-
866 scale metal deposition surveys. Accredit. Qual. Assur. 2, 243–249.
867 Stohl, A., 2006. Characteristics of atmospheric transport into the Arctic troposphere. J.
868 Geophys. Res. Atmos. 111, 1–17. doi:10.1029/2005JD006888
869 Streets, D.G., Devane, M.K., Lu, Z., Bond, T.C., Sunderland, E.M., Jacob, D.J., 2011.
870 All-time releases of mercury to the atmosphere from human activities. Environ.
871 Sci. Technol. 45, 10485–10491. doi:10.1021/es202765m
872 Sturges, W.T., Barrie, L.A., 1989a. Stable lead isotope ratios in Arctic aerosols:

873 evidence for the origin of Arctic air pollution. Atmos. Environ. 23, 2513–2519.
874 doi:10.1016/0004-6981(89)90263-1
875 Sturges, W.T., Barrie, L.A., 1989b. Stable lead isotope ratios in arctic aerosols:
876 evidence for the origin of arctic air pollution. Atmos. Environ. 23, 2513–2519.
877 doi:10.1016/0004-6981(89)90263-1
878 Sturges, W.T., Barrie, L.A., 1987. Lead 206/207 isotope ratios in the atmosphere of
879 North amercia as tracers of US and Canadian emissions. Nature 329, 144–146.
880 Sturges, W.T., Hopper, J.F., Barrie, L.A., Schnell, R.C., 1993. Stable lead isotope ratios
881 in Alaskan Arctic aerosols. Atmos. Environ. Part A. Gen. Top. 27, 2865–2871.
882 Taylor, P.N., Kalsbeek, F., Bridgwater, D., 1992. Discrepancies between neodymium,
883 lead and strontium model ages from the Precambrian of southern East Greenland:
884 Evidence for a Proterozoic granulite-facies event affecting Archaean gneisses.
885 Chem. Geol. 94, 281–291. doi:10.1016/S0009-2541(10)80030-0
886 U.S Geological Survey, 2014. Mercury statistics, in Kelly, T.D., and Matos, G.R comps
887 Historical statistics for mineral and material commodities in the United States
888 United States: U.S. Geological Survey Data Series 140.
889 US Energy Information Administration, 2012. Primary Energy Consumption Estimates
890 by Source (1775-2001) [WWW Document]. Energy Perspect. Fig. URL
891 https://www.eia.gov/totalenergy/data/annual/perspectives.php (accessed 8.15.17).
892 Weiss, D., Shotyk, W., Appleby, P.G., Kramers, J.D., Cheburkin, A.K., 1999.
893 Atmospheric Pb deposition since the industrial revolution recorded by five Swiss
894 peat profiles: Enrichment factors, fluxes, isotopic composition, and sources.
895 Environ. Sci. Technol. 33, 1340–1352. doi:10.1021/es980882q
896 Weiss, D.J., Kober, B., Dolgopolova, A., Gallagher, K., Spiro, B., Le Roux, G., Mason,
897 T.F.D., Kylander, M., Coles, B.J., 2004. Accurate and precise Pb isotope ratio
898 measurements in environmental samples by MC-ICP-MS. Int. J. Mass Spectrom.
899 232, 205–215. doi:10.1016/j.ijms.2004.01.005
900 Whitehouse, M.J., Kamber, B.S., Fedo, C.M., Lepland, A., 2005. Integrated Pb- and S-
901 isotope investigation of sulphide minerals from the early Archaean of southwest
902 Greenland. Chem. Geol. 222, 112–131. doi:10.1016/j.chemgeo.2005.06.004
903 Wu, J., Boyle, E.A., 1997. Lead in the western North Atlantic Ocean: Completed
904 response to leaded gasoline phaseout. Geochim. Cosmochim. Acta 61, 3279–3283.
905 doi:10.1016/S0016-7037(97)89711-6
906 Zheng, J., 2015. Archives of total mercury reconstructed with ice and snow from

907 Greenland and the Canadian High Arctic. Sci. Total Environ. 509–510, 133–144.
908 doi:10.1016/j.scitotenv.2014.05.078
909

105°W

30°E

A

Q

Greenland

A

P

DE

B

Arctic Circle

F

O

T

C

S

G

H

NORTH AMERICA

L

K

J

M

N

EUROPE

I

38°

NORTH ATLANTIC

0 800 1600

Km

R

38°

66°

Nuuk

62°

0 300km

B

N

Nanortalik

C

60°

Sandhavn

Granites

Granites and Migmatites

Metasediments

Gabbros

Ice

Atlantic Ocean

0 15 30

km

45°

44°

Kap Farvel

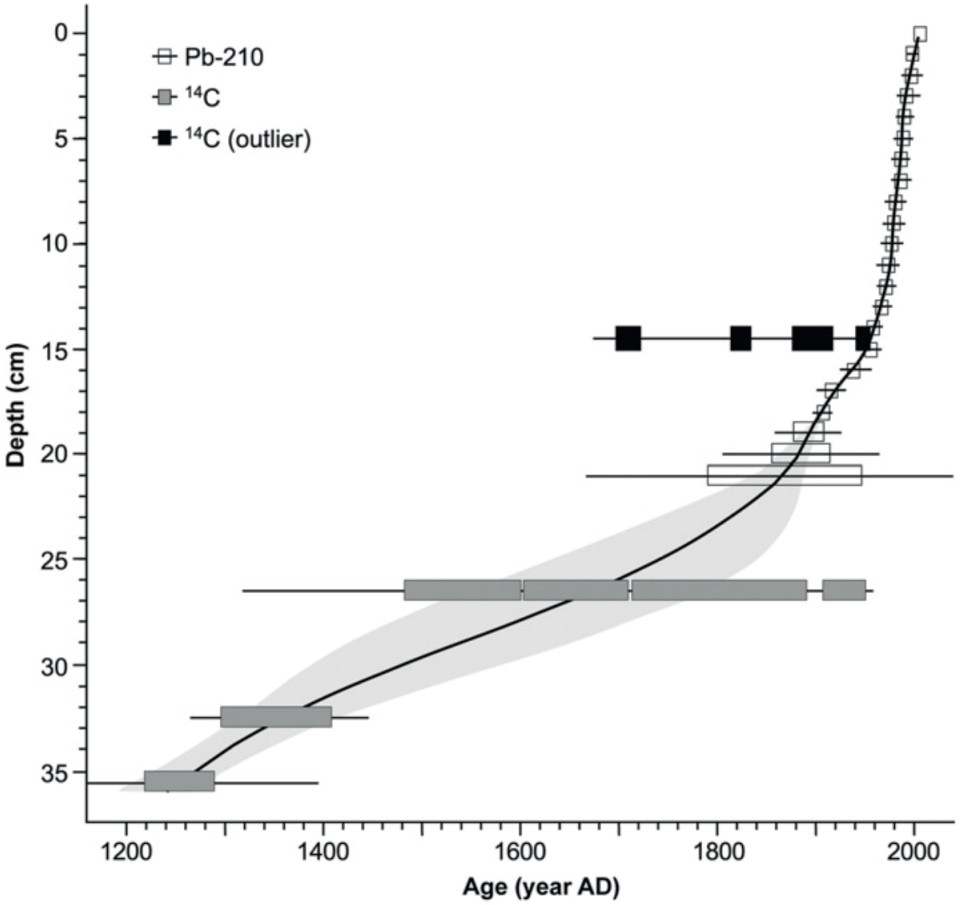
Pb-210
14C
14C (outlier)
Depth (cm)
0
5
10
15
20
25
30
35
1200
1400
1600
1800
2000
Age (year AD)

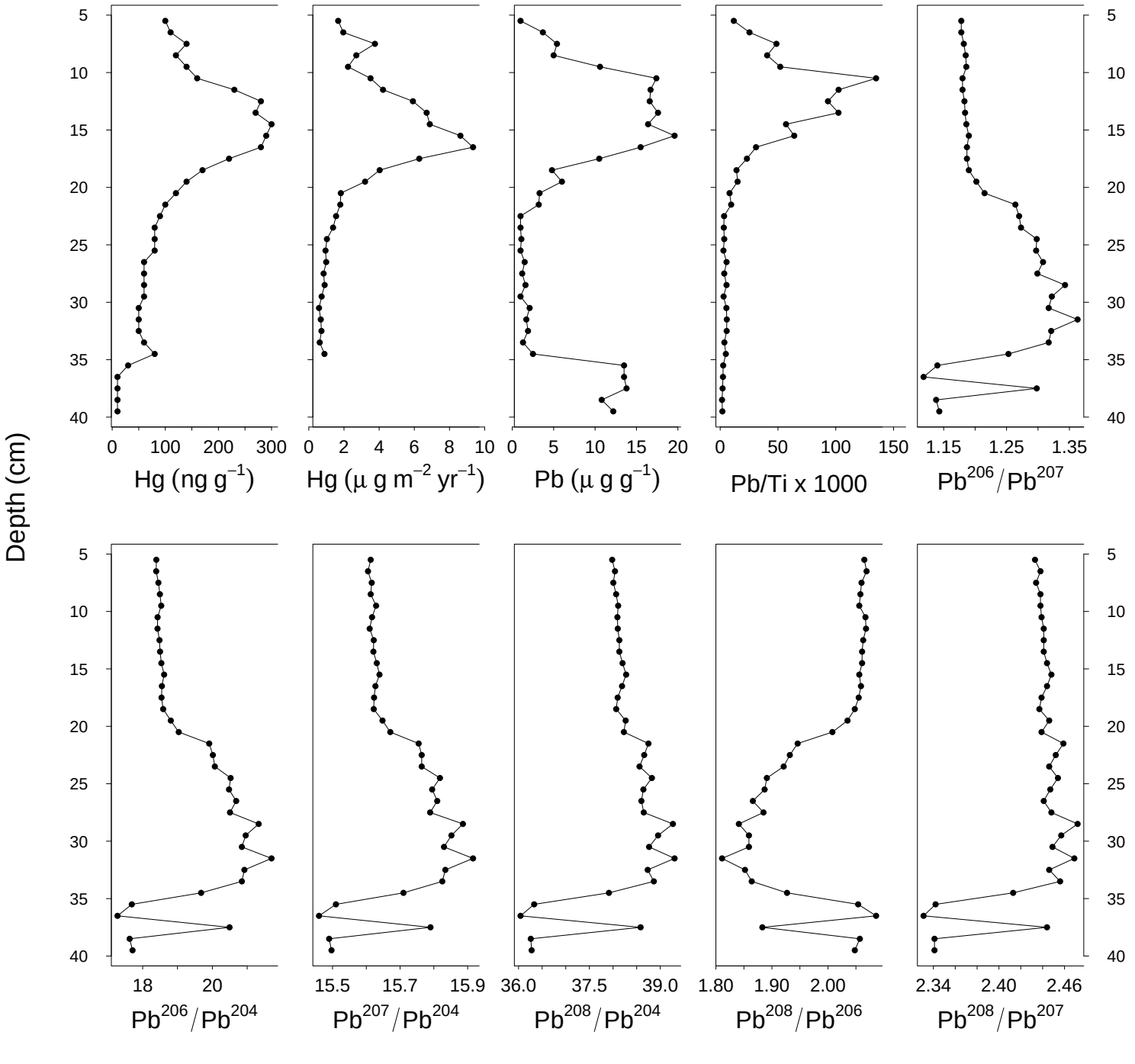
Depth (cm)
5
10
15
20
25
30
35
40
0
100
200
300
Hg (ng g^{-1})
0
2
4
6
8
10
Hg (µ g m^{-2} yr^{-1})
0
5
10
15
20
Pb (µ g g^{-1})
0
50
100
150
Pb/Ti x 1000
1.15
1.25
1.35
Pb^{206}/Pb^{207}
18
20
Pb^{206}/Pb^{204}
15.5
15.7
15.9
Pb^{207}/Pb^{204}
36.0
37.5
39.0
Pb^{208}/Pb^{204}
1.80
1.90
2.00
Pb^{208}/Pb^{206}
2.34
2.40
2.46
Pb^{208}/Pb^{207}

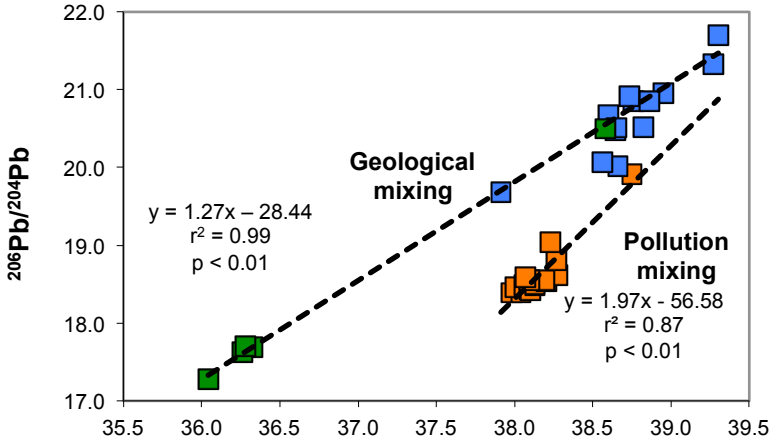
22.0
21.0
20.0
19.0
18.0
17.0
35.5
36.0
36.5
37.0
37.5
38.0
38.5
39.0
39.5
206Pb/204Pb
Geological mixing
y = 1.27x – 28.44
r² = 0.99
p < 0.01
Pollution mixing
y = 1.97x - 56.58
r² = 0.87
p < 0.01

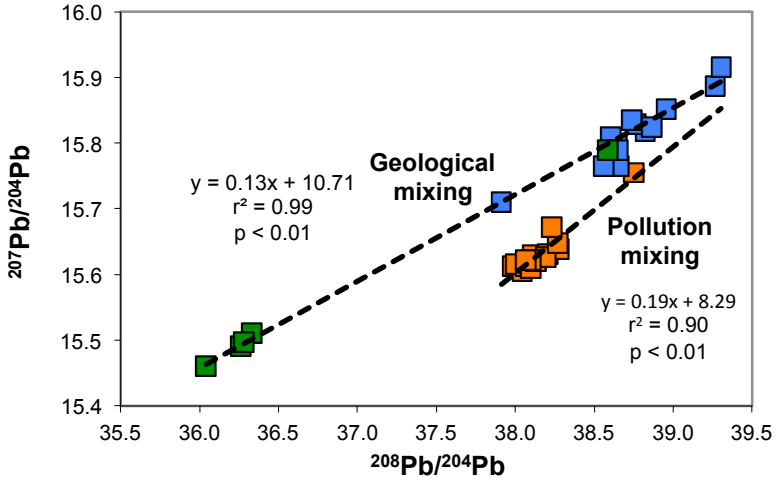
16.0
15.9
15.8
15.7
15.6
15.5
15.4
35.5
36.0
36.5
37.0
37.5
38.0
38.5
39.0
39.5
207Pb/204Pb
208Pb/204Pb
Geological mixing
y = 0.13x + 10.71
r² = 0.99
p < 0.01
Pollution mixing
y = 0.19x + 8.29
r² = 0.90
p < 0.01

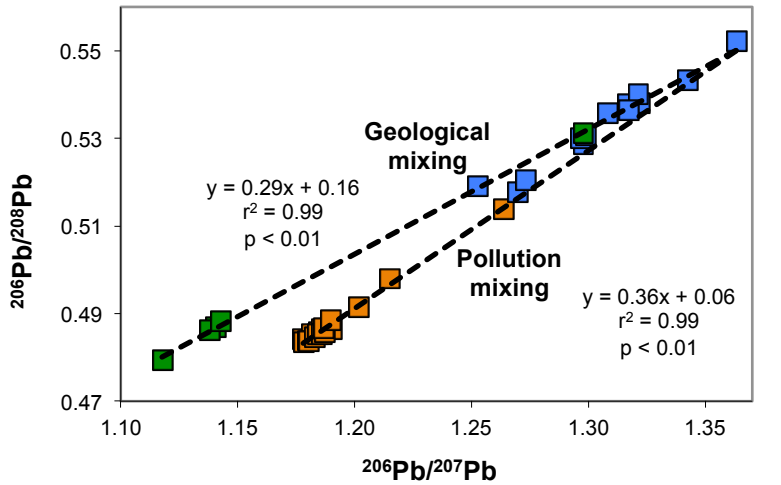
0.55
0.53
0.51
0.49
0.47
1.10
1.15
1.20
1.25
1.30
1.35
206Pb/208Pb
206Pb/207Pb
Geological mixing
y = 0.29x + 0.16
r² = 0.99
p < 0.01
Pollution mixing
y = 0.36x + 0.06
r² = 0.99
p < 0.01

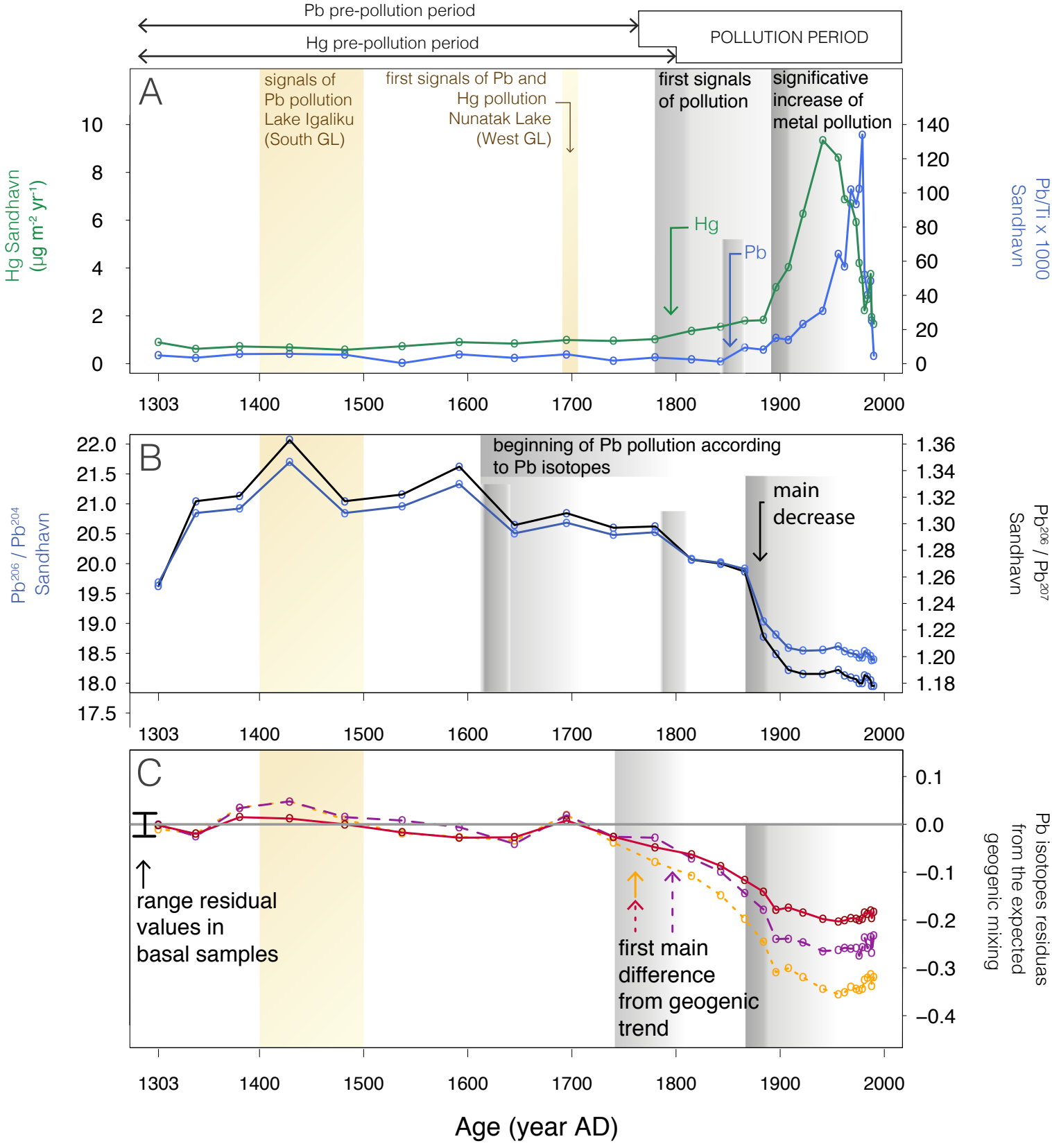
Pb pre-pollution period
Hg pre-pollution period
POLLUTION PERIOD
A
signals of Pb pollution Lake Igaliku (South GL)
first signals of Pb and Hg pollution Nunatak Lake (West GL)
first signals of pollution
significative increase of metal pollution
Hg
Pb
Hg Sandhavn (µg m-2 yr-1)
Pb/Ti x 1000 Sandhavn
B
beginning of Pb pollution according to Pb isotopes
main decrease
Pb206 / Pb204 Sandhavn
Pb206 / Pb207 Sandhavn
C
range residual values in basal samples
first main difference from geogenic trend
Pb isotopes residuas from the expected geogenic mixing
Age (year AD)

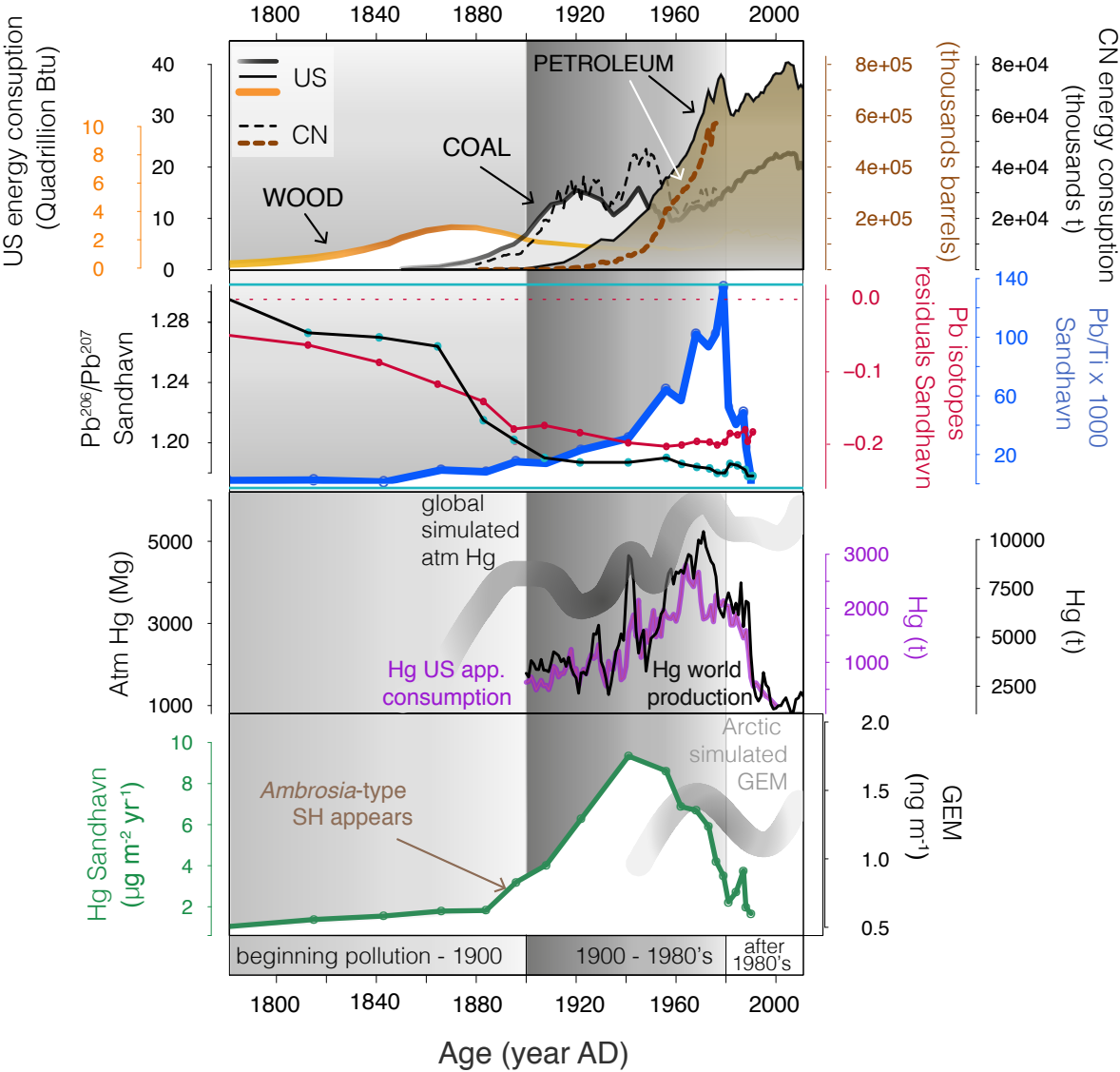
1800
1840
1880
1920
1960
2000
US energy consuption (Quadrillion Btu)
CN energy consuption (thousands t)
US
CN
WOOD
COAL
PETROLEUM
(thousands barrels)
Pb isotopes residuals Sandhavn
Pb/Ti x 1000 Sandhavn
Pb206/Pb207 Sandhavn
Atm Hg (Mg)
global simulated atm Hg
Hg US app. consumption
Hg world production
Hg (t)
Hg Sandhavn (µg m-2 yr-1)
Ambrosia-type SH appears
Arctic simulated GEM
GEM (ng m-1)
beginning pollution - 1900
1900 - 1980's
after 1980's
Age (year AD)

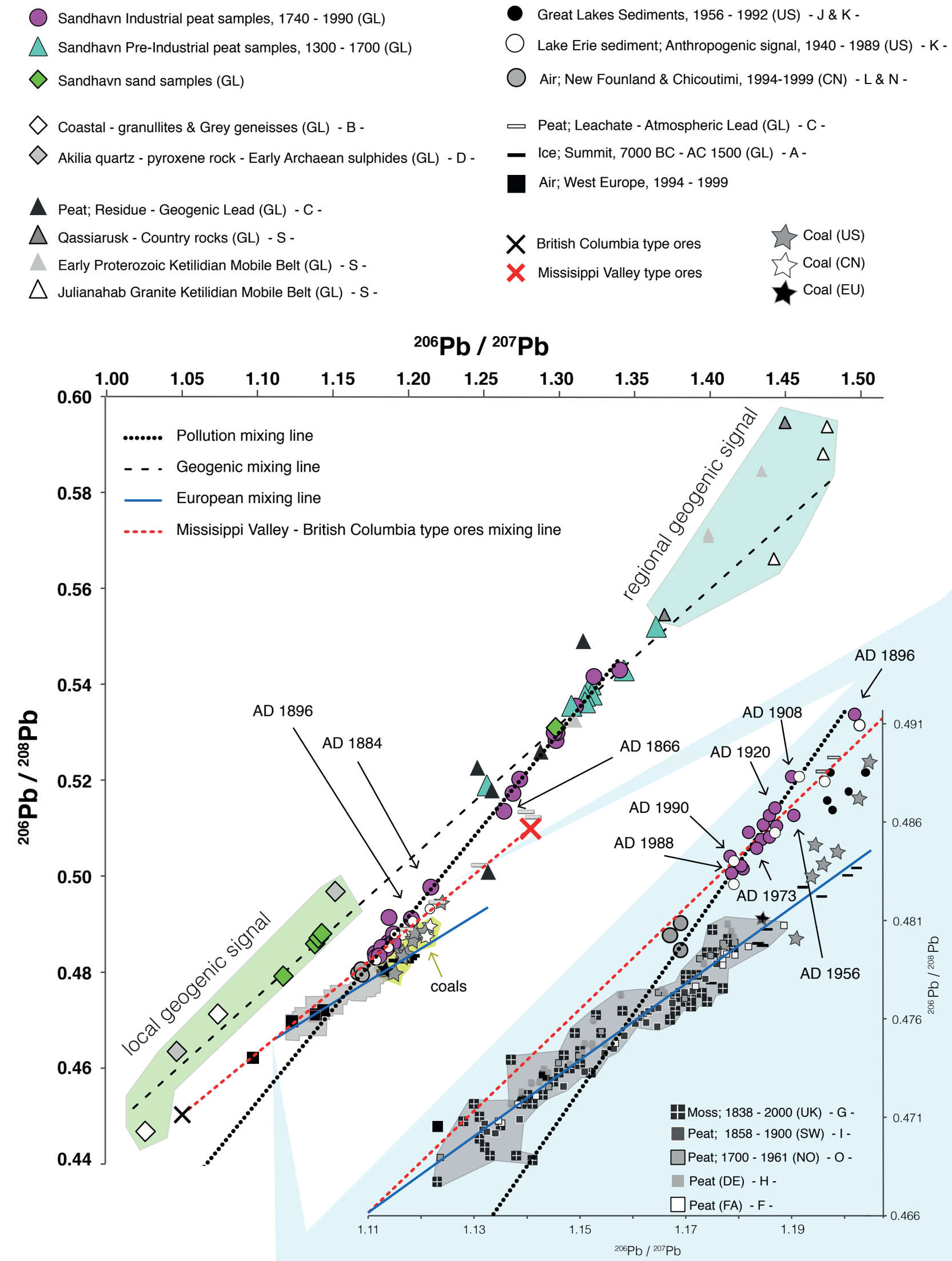
Sandhavn Industrial peat samples, 1740 - 1990 (GL)
Sandhavn Pre-Industrial peat samples, 1300 - 1700 (GL)
Sandhavn sand samples (GL)
Coastal - granullites & Grey geneisses (GL) - B -
Akilia quartz - pyroxene rock - Early Archaean sulphides (GL) - D -
Peat; Residue - Geogenic Lead (GL) - C -
Qassiarusk - Country rocks (GL) - S -
Early Proterozoic Ketilidian Mobile Belt (GL) - S -
Julianahab Granite Ketilidian Mobile Belt (GL) - S -
Great Lakes Sediments, 1956 - 1992 (US) - J & K -
Lake Erie sediment; Anthropogenic signal, 1940 - 1989 (US) - K -
Air; New Founland & Chicoutimi, 1994-1999 (CN) - L & N -
Peat; Leachate - Atmospheric Lead (GL) - C -
Ice; Summit, 7000 BC - AC 1500 (GL) - A -
Air; West Europe, 1994 - 1999
British Columbia type ores
Missisippi Valley type ores
Coal (US)
Coal (CN)
Coal (EU)
206Pb / 207Pb
1.00
1.05
1.10
1.15
1.20
1.25
1.30
1.35
1.40
1.45
1.50
0.60
0.58
0.56
0.54
0.52
0.50
0.48
0.46
0.44
206Pb / 208Pb
Pollution mixing line
Geogenic mixing line
European mixing line
Missisippi Valley - British Columbia type ores mixing line
regional geogenic signal
local geogenic signal
AD 1896
AD 1884
AD 1866
AD 1908
AD 1920
AD 1990
AD 1988
AD 1973
AD 1956
coals
Moss; 1838 - 2000 (UK) - G -
Peat; 1858 - 1900 (SW) - I -
Peat; 1700 - 1961 (NO) - O -
Peat (DE) - H -
Peat (FA) - F -
1.11
1.13
1.15
1.17
1.19
206Pb / 207Pb
0.491
0.486
0.481
0.476
0.471
0.466
206Pb / 208Pb

Supporting Information

Industrial-era lead and mercury contamination in southern Greenland implicates North American sources

Marta Pérez-Rodríguez [1,2 *], Noemí Silva-Sánchez [1], Malin E. Kylander [3,4], Richard Bindler [5], Tim M. Mighall [6], J. Edward Schofield [6], Kevin J. Edwards [6,7,8], Antonio Martínez Cortizas [1]

[1] Departamento de Edafoloxía e Química Agrícola, Facultade de Bioloxía, Universidade de Santiago de Compostela, Campus Sur, Santiago de Compostela 15782, Spain

[2]Institut für Geoökologie, AG Umweltgeochemie, Technische Universität Braunschweig, 38106 Braunschweig Germany

[3] Department of Geological Sciences, Stockholm University, SE-10691 Stockholm, Sweden

[4] The Bolin Centre for Climate Research, Stockholm University, SE-10691 Stockholm, Sweden

[5] Department of Ecology and Environmental Sciences, Umeå University, SE-901 87 Umeå, Sweden

[6] Department of Geography and Environment, School of Geosciences, University of Aberdeen, Elphinstone Road, Aberdeen AB24 3UF, UK

[7] Department of Archaeology, School of Geosciences, University of Aberdeen, Elphinstone Road, Aberdeen AB24 3UF, UK

[8] Clare Hall, University of Cambridge, Herschel Road, Cambridge CB3 9AL, UK

* Corresponding Author:

E-mail: m.perez-rodriguez@tu-bs.de

Current address: Institute of Geoecology - Division of Environmental Geochemistry, Langer Kamp 19c R303B, 38106 Braunschweig Phone: (+)49-(0)531-391-7242

5 Pages

Figure S1. Scatterplot of Hg concentrations against proxies of peat decomposition measured by Silva-Sánchez et al. (2015)

Table S1. Mean (Avg), standard deviation (Sd), maximum (Max) and minimum (Min) values for mercury, lead and lead isotope ratios through the Sandhavn monolith.

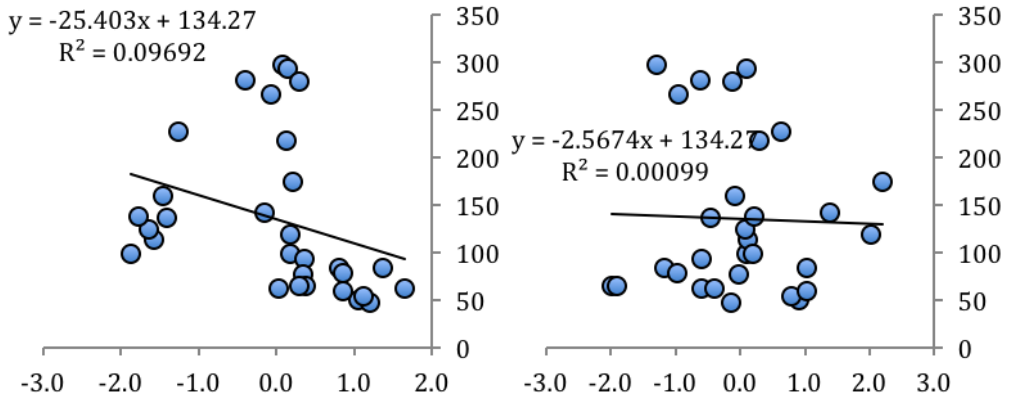

Figure S1. Scatterplot of Hg concentrations against proxies of peat decomposition measured by Silva-Sánchez et al., (2015) (PC1o, left panel; PC3o, right panel) in the Sandhavn record. The p-values of Pearson's test are 0.09 and 0.88 respectively.

Table S1. Mean (Avg), standard deviation (Sd), maximum (Max) and minimum (Min) values for mercury, lead and lead isotope ratios through the Sandhavn monolith.

		Hg (ng g^{-1})	Acc Hg (µg m^{-2} yr^{-1})	Pb (µg g^{-1})	Acc Pb (µg m^{-2} yr^{-1})	Pb^{206}/Pb^{204}	Pb^{207}/Pb^{204}	Pb^{208}/Pb^{204}	Pb^{206}/Pb^{207}	Pb^{206}/Pb^{208}
Peat	**Avg**	134	2.88	6.3	144.8	19.508	15.712	38.416	1.241	0.508
	Sd	81.6	2.54	6.6	174.5	1.115	0.101	0.392	0.063	0.024
	Max	297	9.34	19.6	577.9	21.699	15.916	39.302	1.363	0.522
	Min	47	0.58	0.1	1.3	18.389	15.605	37.913	1.178	0.483
Sand	**Avg**	14	-	12.8	-	18.160	15.549	36.698	1.167	0.494
	Sd	7.8	-	1.2	-	1.316	0.136	1.060	0.074	0.02
	Max	28	-	13.8	-	20.494	15.790	38.583	1.298	0.531
	Min	9	-	10.8	-	17.278	15.460	36.042	1.118	0.479

References

Silva-Sánchez, N., Schofield, J.E., Mighall, T.M., Martínez Cortizas, A., Edwards, K.J., Foster, I., 2015. Climate changes, lead pollution and soil erosion in south Greenland over the past 700 years. Quat. Res. 84, 159–173. doi:10.1016/j.yqres.2015.06.001